

## Patient-Specific Image-Based Computational Modeling in Congenital Heart Disease: A Clinician Perspective

Miguel Silva Vieira, Tarique Hussain, Carlos Alberto Figueroa

Miguel Silva Vieira, Tarique Hussain, Carlos Alberto Figueroa, Division of Imaging Sciences & Biomedical Engineering, The Rayne Institute, King's College London, Guy's & St Thomas' NHS Foundation Trust, the United Kingdom

Tarique Hussain, Division of Imaging Sciences & Biomedical Engineering, The Rayne Institute, King's College London, Guy's & St Thomas' NHS Foundation Trust/ Evelina Children's Hospital, the United Kingdom

Carlos Alberto Figueroa, Departments of Surgery and Biomedical Engineering, University of Michigan, Ann Arbor, MI, the United States

Correspondence to: Miguel Silva Vieira, MD, Division of Imaging Sciences & Biomedical Engineering, The Rayne Institute, King's College London, 4th Floor, Lambeth Wing, St. Thomas' Hospital, London SE1 7EH, the United Kingdom

Email: [miguel.silvavieira@kcl.ac.uk](mailto:miguel.silvavieira@kcl.ac.uk)

Telephone: +44 (0)20 7188 7242 Fax: +44 (0)20 7188 5442

Received: July 18, 2015 Revised: September 15, 2015

Accepted: September 20, 2015

Published online: December 10, 2015

### ABSTRACT

Despite major advances in the understanding of congenital heart disease, the clinical decision-making process is still based on consensus opinion of experts, small prospective and retrospective studies, or registries. Furthermore, because the decision process is mainly supported by empirical data from cohorts of patients with similar conditions, it might not reflect the individual subject nor does it allow making predictions on the outcome in response to a variety of therapeutic options. In response to this need, the new paradigm of "predictive personalized medicine" postulates the use of computational tools that integrate patient-specific medical imaging (as well as other measurements) to simulate and quantify physiologic and pathophysiologic function of the cardiovascular system. The ultimate goal is to perform a subject-specific hemodynamic assessment and, when applicable, to predict the outcome of alternative treatment plans for an individual patient. In this article, we review image-based

computational modeling in congenital heart disease. We remark that closer interactions between bioengineers and clinicians, and dedicated cross-disciplinary training are crucial to bridge the gap between image-based modeling and daily clinical scenarios.

© 2015 ACT. All rights reserved.

**Key words:** Congenital heart disease; Computational modeling; Cardiovascular imaging

Vieira MS, Hussain T, Figueroa CA. Patient-Specific Image-Based Computational Modeling in Congenital Heart Disease: A Clinician Perspective. *Journal of Cardiology and Therapy* 2015; 2(6): 436-448 Available from: URL: <http://www.ghrnet.org/index.php/jct/article/view/1512>

### Abbreviations

A: area;  
C: compliance;  
CAD: computer-aided design;  
CBF: coronary blood flow;  
CFD: computational fluid dynamics;  
CHD: congenital heart disease;  
CMR: cardiovascular magnetic resonance;  
CO: cardiac output;  
CoA: aortic coarctation;  
CT: computed tomography;  
 $\Delta P$ : pressure change;  
 $\Delta V$ : volume change;  
E: stiffness;  
 $\epsilon$ : strain;  
F: force;  
FDA: Food and Drug Administration;  
HLHS: hypoplastic left heart syndrome;  
HPC: high performance computing;  
L: vessel length;  
LV: left ventricle;

$\mu$ : blood viscosity;  
 $\sigma$ : (circumferential);  
 NURBS: non-uniform rational b-spline;  
 P: pressure;  
 PC: phase-contrast;  
 PPS: peripheral pulmonary stenosis;  
 PWS: peak wall stress;  
 r: radius;  
 RV: right ventricle;  
 WSS: wall shear stress.

## INTRODUCTION

In the last 60 years, there has been a major improvement in the life expectancy of patients with congenital heart disease (CHD). Previously, only about 20% of these patients would reach adulthood. However, successful pediatric cardiology programs (with improved early diagnosis) and pediatric cardiac surgery breakthroughs have allowed that nowadays over 85% of young adults with CHD have nearly similar life expectancy as their peers without congenital cardiovascular malformations<sup>[1]</sup>. These advances in diagnosis and surgical treatment have consequently led to an increasing prevalence of patients with CHD in the general population. Furthermore, more careful diagnosis and more sensitive measurements have shown higher prevalence of residual and associated defects in patients with CHD. Indeed, recent data has revealed an increasing complexity and comorbidities of CHD patients surviving into adulthood, further stressing the need for personalized care<sup>[2]</sup>.

Despite the major advances in the care of CHD patients, the clinical decision-making process is still based on consensus opinion of experts, small prospective and retrospective studies, or registries. The lack of supporting data determines that the majority of the guidelines for the management of grown-up congenital heart disease patients have the lowest evidence level (level C)<sup>[3-5]</sup>. Additionally, the safety and effectiveness of most drugs or procedures have not been formally studied in children. Although largely off-label, clinicians have often used medicines and treatments based on what is known to work in adults, which poses a significant risk to a particularly vulnerable subset of patients<sup>[6]</sup>. Not only pharmacokinetic and pharmacodynamic properties of certain drugs may differ considerably in children from their adult counterparts, but also extrapolating empirical data on treatments from cohorts of patients with similar conditions, might not reflect the individual subject.

With other ancillary diagnostic tools, imaging and particularly functional imaging plays a crucial role in understanding the complex anatomic malformations and the resultant pathophysiologic adaptations in these patients, underpinning an initial clinical diagnosis. The remarkable improvements in the diagnostic assessment and accurate treatment decisions rely more and more on precise and detailed information provided by the multiple sophisticated imaging modalities available<sup>[3,4,7]</sup>. Moreover, multidimensional image data provides the ability to customize biomechanical and physiological parameters to a particular patient's anatomy, integrating models of cardiac and vascular physiology. These integrative models of cardiovascular pathophysiology are key for the understanding of disease and for management/intervention planning. Nevertheless, in the overall diagnostic workup of certain defects or diseases, clinicians still rely on the "gold-standard" information from invasive, riskier hemodynamic assessment<sup>[8]</sup>.

Cardiac output (CO) for instance, one of the most important physiological parameters that reflects the metabolism of the entire body

and its ability to adapt to changes in workload, requires accurate quantification in the assessment of intra-cardiac shunts or during right heart catheterization to determine resistance in pulmonary hypertension studies. However, "gold-standard" invasive methods like Fick's and thermodilution techniques are not completely accurate for measuring CO in all patients (e.g. thermodilution method tends to overestimate the CO in the presence of low outputs) and make various key assumptions on the physiologic state of the subject (e.g., accurate oxygen consumption measurements and the inability to obtain a steady state under certain conditions are known drawbacks of Fick's methodology). Additionally, these methodologies can only provide physiological assessment at a limited number of spatial locations.

In this manuscript we will discuss the current state of image-based modeling applications in the medical field, from disease research, to medical device design and performance evaluation, to virtual surgical planning, focusing on CHD problems.

## IMAGING AND COMPUTATIONAL METHODS IN CONGENITAL HEART DISEASE

Patient-specific computational modeling requires accurate three-dimensional (3D) anatomical and physiological models derived from advanced medical imaging, rather than simplified geometric approximations of the anatomy with idealized flow and pressure conditions. Sophisticated multimodality cardiovascular imaging enables the definition of the computational domain (e.g. the anatomy), the boundary conditions (e.g. measurements of flow and pressure), as well as the tissue function and properties. In this section, we provide an overview of the different imaging and computational tools necessary for simulation of cardiovascular dynamics.

### 1. Acquisition of morphologic and physiologic data using medical imaging

The current non-invasive techniques that allow simultaneous characterization of cardiovascular anatomy and hemodynamics are Doppler echocardiography, computed tomography (CT) and cardiovascular magnetic resonance (CMR).

Even though two-dimensional (2D) echocardiography is still the first-line tool for diagnostic assessment of these patients, the intricate nature of some cardiovascular malformations requires a broader bird's-eye view. The comprehensive nature of the non-invasive cross-sectional imaging modalities, particularly of CMR, has enabled to perform accurate and high-spatial resolution 3D anatomical reconstructions, with increasing temporal resolution to depict flow dynamics<sup>[9]</sup>.

Although not a new technology and originally used in engineering and car industry to generate prototype models, the use of 3D printing techniques to create cardiovascular models based on these detailed imaging modalities has received renewed attention from both the medical community and media (Figure 1). This technique has been shown to contribute both to the pre-operative surgical planning in complex congenital cardiovascular defects and also to help fabricate customized implants that can be tested before surgery<sup>[10]</sup>.

It is beyond the scope of this article to provide a comparison between all available imaging modalities, since currently no one provides anatomically and physiologically accurate data at all phases of patient care, from the fetal stage onwards. Moreover, caution is required when comparing different modalities due to the discrepancies between the quantities measured (e.g. Doppler ultrasound measures the peak velocity within a voxel while each voxel in CMR provides an estimate of the mean velocity).

*Doppler echocardiography*

Doppler echocardiography provides a useful and inexpensive bedside screening tool to study flow patterns, function and myocardial velocities<sup>[11]</sup>. 2D echocardiography is still the best modality in terms of temporal resolution, enabling to capture specific features of cardiac dynamics. Reconstruction algorithms using acquired conventional 2D color-Doppler data have been used to depict the intra-ventricular flow maps with high temporal resolution thus allowing characterization of the complex ventricular vortex flows, assessment of myocardial efficiency and kinetic energy dissipation, and estimating 2D pressure maps<sup>[12]</sup>. Extensively validated in the assessment of pressure gradients in acquired cardiovascular diseases, these pressure gradients are calculated using simplified Bernoulli principles, under a planar blood flow assumption, with the added error of potential user-dependent scan-plane misalignment during ultrasound beam interrogation. Furthermore, Doppler ultrasound cannot resolve a velocity map on a randomly oriented anatomic plane of the acquired domain.

Not surprisingly, the accuracy and reliability of some of these measurements is still debated. This is particularly true in the assessment of the left ventricle (LV) filling pressure and pulmonary pressure<sup>[13,14]</sup>. Although several proposed Doppler echocardiographic indexes have been discredited by conflicting evidence, they still provide valuable insights into the pathophysiology of both right and left ventricular adaptations and ventriculo-arterial mechanics<sup>[15]</sup>.

Recently, 3D echocardiography has been shown to overcome the major limitation of 2D angle-dependent Doppler-based measurements by allowing the calculation of angle-independent 3D intracardiac velocity vectors. This 3D echocardiographic data could be used to provide more sophisticated boundary conditions for simulation studies<sup>[16]</sup>.

*Computed tomography*

Modern CT commercial scanners allow sub-millimeter in-plane spatial resolution and increasingly higher temporal resolution for gated imaging, due to the fast gantry rotations achieved and the advanced iterative reconstruction algorithms used. This has allowed to acquired highly resolved images with relatively low-dose radiation, a particular relevant topic in pediatrics given the stochastic effect of cumulative exposure to radiation and cancer risk<sup>[17]</sup>. Advances in computational fluid dynamics (CFD) now enable calculation of coronary flow and pressure fields from CT-derived anatomical image data. This allows for the functional assessment of coronary plaque disease, obtaining maps of coronary wall shear stress (WSS), the tangential force generated by the friction of flowing blood on the endothelial surface of the arterial wall, which is correlated with plaque destabilization and rupture<sup>[18]</sup>. It is also possible to non-invasively determine the significance of coronary artery stenosis using entirely image-based computational methods, thus saving the patients from an invasive diagnostic catheterization<sup>[19]</sup>.

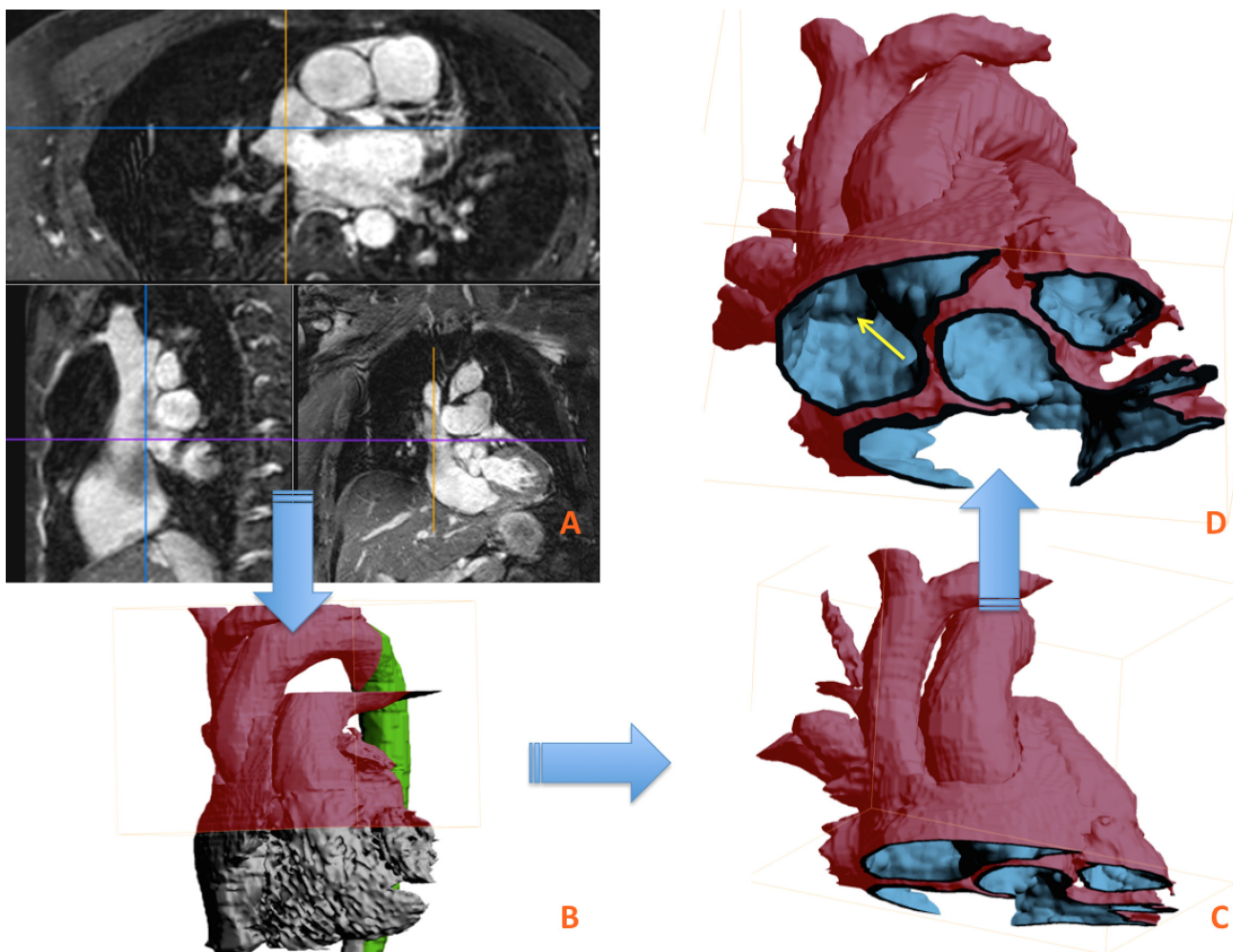


**Figure 1** Panels A to C. Segmentation process of a 3D balanced steady-state free precession CMR dataset from a patient with superior sinus venosus atrial septal defect (ASD). Panel D. Orthogonal inferior perspective of the ASD after a customizable cutting plane through the middle of the heart, to allow 3D visualization of the defect. An imaged-based cast can be printed out to help tailor the best intervention for this patient.

However, CT assumes universal form–function relationships or allometric scaling laws relating the mass of an object to shape and size, anatomy, and physiology to estimate the blood flow rate<sup>[19]</sup>. An example is the estimation of the total coronary blood flow (CBF) at rest, which is assumed to be proportional to myocardial mass. Since the myocardial mass can be calculated from the volumetric CT angiography data, one can extrapolate the CBF using these form–function relationships<sup>[19,20]</sup>.

#### Cardiovascular magnetic resonance

CMR allows simultaneous acquisition of high spatial and high temporal resolution anatomic data and 3D velocity maps of blood flow, not limited by acoustic window or patient body surface area. The possibility of obtaining temporal-spatial velocity maps permits a direct examination of blood velocities, flow rate and even WSS throughout the cardiac cycle. The key advantage of velocity encoded phase-contrast (PC) CMR techniques is that, in addition to measuring velocity in any imaging plane, the area of the vessel of interest is also captured simultaneously, allowing for volume of flow to be accurately calculated<sup>[21]</sup>. Additionally, new 4D flow sequences offer further advantages over 2D methods, enabling retrospective analysis of flow in any location in the imaging volume. 4D flow has been recently applied to study flow patterns in severe pulmonary hypertension: it has been observed that flow changes from a laminar to a helical/vortex pattern with different diastolic streamlines<sup>[22]</sup>. These swirling flow patterns can result in inaccuracies when assessed by 2D through-plane flow techniques.

## 2. Engineering analysis and modeling

Models are an approximation of reality that helps to understand function. In engineering, modeling has traditionally relied on using complex partial differential equations (such as the Navier-Stokes equations) to describe a certain physical phenomenon. These equations can be solved either analytically or numerically. Analytical solutions (such as Poiseuille's law) can be obtained under a series of simplified conditions on the physics and geometry (for instance, steady flow in a perfectly cylindrical rigid tube), and provide a closed-form solution for the quantity of interest. These assumptions (e.g. non-deformable tubes) entail obvious limitations when applied to dynamic problems/systems such as the human vessels. On the other hand, when the combination of physics and anatomy is complex (for instance, turbulent 3D flow through a stenotic vessel), there are no analytical solutions that can accurately describe the physics. Indeed, in aortic coarctation (CoA) for instance, flow is highly 3D and significant viscous losses occur as blood moves through the stenotic area. Under these conditions, the simplified Bernoulli's law, commonly used in cardiovascular medicine and which assumes no viscous dissipation, is fundamentally flawed. An accurate, non-invasive estimation of the pressure gradient can only be obtained by solving the complex partial differential equations (e.g. Navier-Stokes), using numerical techniques and high performance computing (HPC).

In the following, we provide an overview of several fundamental closed-form solutions that are commonly used to gain basic insight on the mechanics of blood flow and vessel wall dynamics<sup>[23,24]</sup>. Then, we will provide a simple overview of the computational modeling workflow, specifically focused on CFD applications.

### 2.1. Fundamental solutions for blood flow and cardiovascular mechanics

The cardiovascular circulation is a closed-loop, pulsatile system. The heart, a myogenic organ, pumps blood at every cardiac cycle

throughout the systemic and pulmonary circulations in a pulsatile manner. The motion of blood can be described mathematically as an incompressible fluid (with constant or shear-dependent viscosity) governed by the so-called Navier-Stokes equations, which describe the conservation of linear momentum and mass. The Navier-Stokes equations describe the fluid motion in three spatial dimensions, due to forces such as pressure gradients, viscous losses, acceleration, and gravity. Because of their nonlinear character, obtaining a solution to these equations requires the use of HPC and numerical methods. A number of simplifications to the 3D Navier-Stokes equations have been utilized to describe flow and pressure under much simpler terms.

#### The Windkessel model

One of the most commonly used simplified models of the circulation is the so-called “lumped-parameter models”, which consists of electric analogues of the circulation. The Windkessel model described by Otto Frank in the late 19th century, was the first lumped-parameter model (Figure 2). It was designed to represent the heart and the systemic arterial system in terms of an aortic inflow pressure-flow relationship, assuming known values of resistance and compliance of a distal vascular bed, similar to a hydraulic circuit<sup>[25]</sup>. The model explains the exponential decay in diastolic aortic pressure following aortic valve closure, and can estimate the workload on the heart in terms of peripheral resistance and total arterial compliance<sup>[26]</sup>. Windkessel models have also been widely used to characterize parameters such as arterial compliance, peripheral resistance and as a mean to derive aortic flow or arterial pressure from image data<sup>[27]</sup>.

Lumped parameter models can have different designs: from 2-element models that take into account the arterial compliance and total peripheral resistance, to 3 or 4-element models that provide a finer description of the distal vascular bed.

#### Poiseuille's law

Another commonly utilized simplified model of the circulation is given by Poiseuille's law (Figure 3). Poiseuille's law provides an analytical solution for the Navier-Stokes equations under the assumptions of steady flow in a symmetric, cylindrical vessel, in the absence of gravity, and under a constant pressure gradient (Figure 4). Poiseuille's law

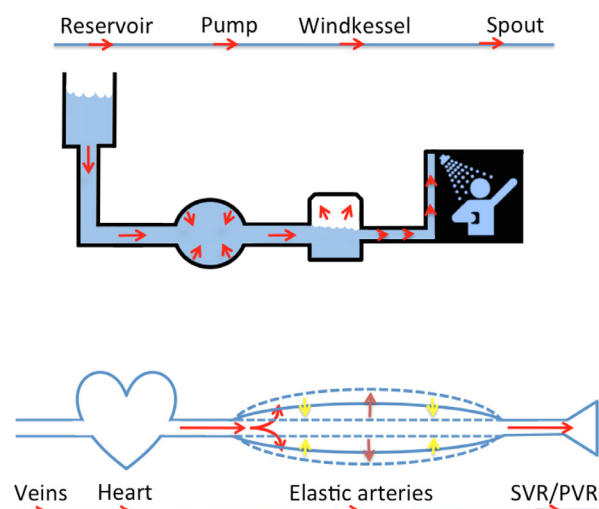


**Figure 2** Representation of the Windkessel model of the human circulation with the correspondent and equivalent hydraulic system<sup>[26]</sup>. The Windkessel is similar to a water pump connected to a chamber, filled with water but with a pocket of air. As the water is pumped, it compresses the air, pushing water out of the chamber.



relates flow to a constant pressure gradient and a resistance that is directly proportional to the vessel length ( $L$ ), the blood viscosity ( $\mu$ ), and inversely proportional to the fourth power of the vessel radius ( $r$ ).

#### Laplace's law

Laplace's law is another commonly used analytical solution in CFD. It applies to cylindrical (vessels) or spherical (ventricular chamber) geometries, whether the material has linear or nonlinear mechanical properties and irrespective of wall thickness. It states that wall stress is directly proportional to the product of the luminal pressure and the radius and inversely proportional to the wall thickness (Figure 5).

#### Vascular stiffness and compliance

Stiffness ( $E$ ) is the relationship between stress ( $\sigma$ ) and strain ( $\epsilon$ ):  $E = \sigma/\epsilon$ . Graph 1 in figure 6 shows two materials (A and B) with different stiffness:  $E_1$  and  $E_2$ . The material with the steepest slope in the stress-strain curve behaves in a stiffer way. The heart and blood vessels exhibit a nonlinear relationship between stress and strain. At lower levels of stress (i.e., lower pressures) the tissue behaves in a compliant way (i.e., larger strains for a given increment in pressure). However, as stress goes up, the tissue behaves in a stiffer and stiffer way (curve C, graph 1 of Figure 6). This is explained by the behavior of the different constituents of the arterial tissue: at lower stress, the elastin fibers, which are compliant, dominate. Conversely, the collagen fibers (much stiffer in nature) dominate at high values of stress<sup>[28]</sup>.

Compliance ( $C$ ) is defined as a change in volume ( $\Delta V$ ) for a given change in pressure ( $\Delta P$ ), i.e.  $C = \Delta V/\Delta P$ . It is a fundamental property of the heart and blood vessels, which can be altered due to histological changes in the tissue. The compliance curve shows a nonlinear relationship between volume and pressure. This means that when the tissue is exposed to higher pressures, it experiences smaller changes in volume for a given change in pressure (Figure 6, graph 2)<sup>[29]</sup>.

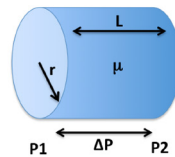
All these solutions/metrics don't suffice in complex anatomical and physiological configurations. For these, no analytical solutions can be accurately applied and one must resort to computational tools such as CFD to describe the physics at hand. In the next section, we provide an overview of typical applications of CFD in the cardiovascular field.

## 2.2. Computational fluid dynamics in cardiovascular medicine

CFD is a discipline that uses numerical methods and algorithms to solve the Navier-Stokes equations of conservation of mass and momentum to describe and solve fluid problems. Although it was first used in traditional engineering areas such as chemical, aerospace/aeronautic and the automotive industry, it has recently emerged as a valuable tool in biomedical engineering research<sup>[30]</sup>. The ever-increasing CFD applications in cardiovascular research span from understanding the pathophysiology in certain diseases, acquired or congenital, to developing new and improved medical devices, or to the optimization of existing procedures through computer simulations, resulting in enhanced efficiency and lower costs<sup>[29]</sup>.

#### Cardiovascular disease research

The application of image-based CDF tools to medicine started essentially in the early nineties. In a landmark study, Gonzalez and co-workers tried to understand the factors determining the origin and progression of intracranial aneurysms and their risk of rupture using the hemodynamic data obtained from computer simulations<sup>[31]</sup>. However, only in the late nineties did CFD take off as a powerful tool to study hemodynamics in numerous vascular territories, in both occlu-

$$Q = \frac{\pi r^4 \Delta P}{8 \mu L} \rightarrow Q \rightarrow \text{Resistance} = \frac{8 \mu L}{\pi r^4}$$


**Figure 3** Poiseuille's Law for a hydraulic system describing the behavior of fluids through pipes can be used to describe the flow of blood through the arteries. Poiseuille's law describes the rate of flow (the volume of fluid passing a certain point along the tube per second) in terms of the fluid's viscosity, the vessel's radius and length, and the pressure difference along the tube. Resistance is directly proportional to viscosity and inversely proportional to the fourth power of the radius. Therefore, given the relationship between resistance and radius, it is clear that the majority of the vascular resistance is concentrated at the level of the pre-capillary arterioles (diameter <150 μm). Q, flow; r, radius; ΔP, pressure difference (P1 high-pressure to P2 low-pressure); μ, blood viscosity; L, length of the tube.

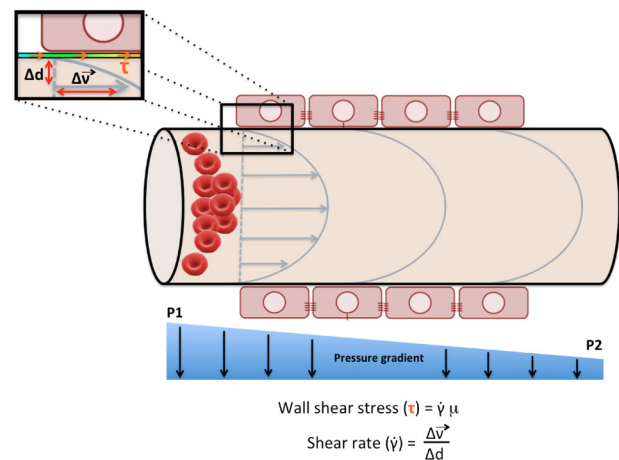
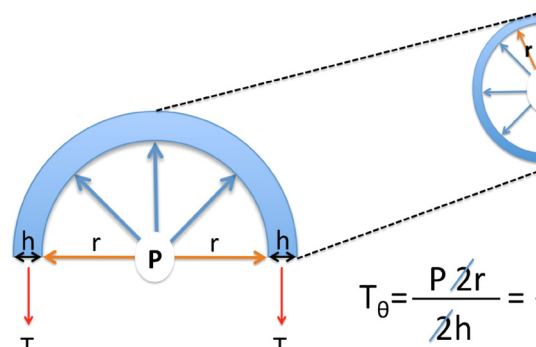


**Figure 4** Schematic of a longitudinal section of a tube representing an idealized arterial vessel. Poiseuille's analytical solution for an incompressible (no change of volume), Newtonian fluid (constant viscosity) assumes constant flow (no acceleration) in a rigid (non-deformable) cylindrical tube, with constant cross-sectional area and a constant pressure gradient driving the flow. Under these assumptions, Poiseuille's solution produces a parabolic velocity profile as depicted in the figure, with a zero velocity at the vessel wall boundary and maximum axial velocity at the center of the vessel. Because of these assumptions, there are obvious limitations to its use for the understanding of biofluids and vessel wall mechanics. However, such analytical solutions allow us to derive important parameters that have been correlated with important clinical outcomes (e.g. tensile stress and risk of aneurysm rupture, endothelial shear stress and coronary atherosclerotic plaque and vascular remodeling). The shear rate at the inner wall of a Newtonian fluid flowing within a pipe is given by the ratio between the linear fluid velocity ( $v$ ) and the diameter of the pipe ( $d$ ). Wall shear rate is related to the shear rate by multiplying it by the fluid viscosity ( $\mu$ ).



$$T_{\theta} = \frac{P \cdot 2r}{2h} = \frac{P \cdot r}{h}$$

**Figure 5** Laplace's law schematic.  $T_{\theta}$ , wall tensile (circumferential) stress; P, transmural pressure; r, radius; h, wall thickness.

sive and aneurysmal disease<sup>[32]</sup>. Due to recent advances in computer science, improved accessibility to HPC and better software, these numerical simulations techniques can now be used to study patient-specific hemodynamics in a variety of healthy and diseased scenarios<sup>[33]</sup>.

#### Medical device design

Manufacturers soon realized about the potential of CFD as a tool to push forward computer-guided design of devices. For instance, coronary stent manufacturers are now using CFD to assess the hemodynamic effects of stent design and strut geometry and their correlation with parameters such as the distribution of WSS on the vessel wall of the stented coronary arteries. WSS is known to be a factor in the development of atherosclerotic plaques and is also thought to play a role in stent restenosis. Because WSS and other local parameters of altered hemodynamics are difficult to measure *in vivo*, computational modeling can be used, alongside with experimental data, to gain insight on different aspects of stent design that may reduce the risk of vascular injury and subsequent restenosis<sup>[34]</sup>.

#### Virtual surgical planning

A growing body of evidence is showing how a new virtual reality approach for cardiac interventions can be useful in complex CHD<sup>[35]</sup>. Cardiovascular experimental models can be particularly informative for device testing (e.g., stent migration, test a range of artificial shunt lengths and diameters to predict hemodynamics in a Fontan circulation). Additionally, CFD simulations have been utilized to understand the hemodynamic effects of a number of surgical operations, including staged reconstruction of the single ventricle physiology.

The use of numerical simulations to evaluate and predict hemodynamic results of performing either an hybrid or a surgical Norwood palliation in hypoplastic left heart syndrome (HLHS), exemplifies the uniqueness of this investigative tool in CHD<sup>[36]</sup>. The hybrid procedure, using a combination of both transcatheter and surgical approaches, attains the goals of Stage I palliative repair without the detrimental effects of prolonged neonatal cardiopulmonary bypass

and hemodynamic instability post circulatory arrest. Although this has gained popularity in patients who were considered high-risk for the surgical Norwood palliation, there is still limited evidence comparing the outcomes of both procedures. Furthermore, the available retrospective data highlights that the final choice is mainly based on surgeon's and institution experience and preference<sup>[37]</sup>.

Validated multiscale computational models have been use to quantify the hemodynamics and parameters such as systemic oxygen delivery, allowing to compare the reconstructed circulations of both palliative procedures for HLHS<sup>[38]</sup>. Recent work has shown that the hybrid approach results in poorer hemodynamic palliation compared with the Norwood Stage I operation<sup>[37]</sup>. Before results from randomized clinical trials become available to provide outcome data, CFD can provide unique patient-specific mechanistic insights into these complex congenital malformations. These can be interpreted as an extra piece of evidence upon which clinicians can support their management decisions.

### IMAGE-BASED COMPUTATIONAL MODELING WORKFLOW FOR CLINICIANS

Virtual prototyping, now the standard method to develop new products in a number of industries such as the automotive, has also been rapidly accepted in some areas of medicine such as orthopedics and orthodontic treatment. However, despite the remarkable breakthroughs in cardiovascular medicine over the past decades, customization of surgical techniques and medical devices in cardiovascular medicine still relies in a cumbersome, costly test-driven approach, involving pre-clinical testing, randomized multicenter clinical trials with hard clinical end-points, and post-marketing surveillance for evaluation of patients outcomes to judge success<sup>[39]</sup>. There is therefore a pressing need to supplement the current test-driven paradigm in cardiovascular medicine with a more cost-effective and streamlined virtual testing paradigm. This is particularly the case when dealing with rare conditions, where recruiting enough patients to provide robust clinical evidence may not be feasible.

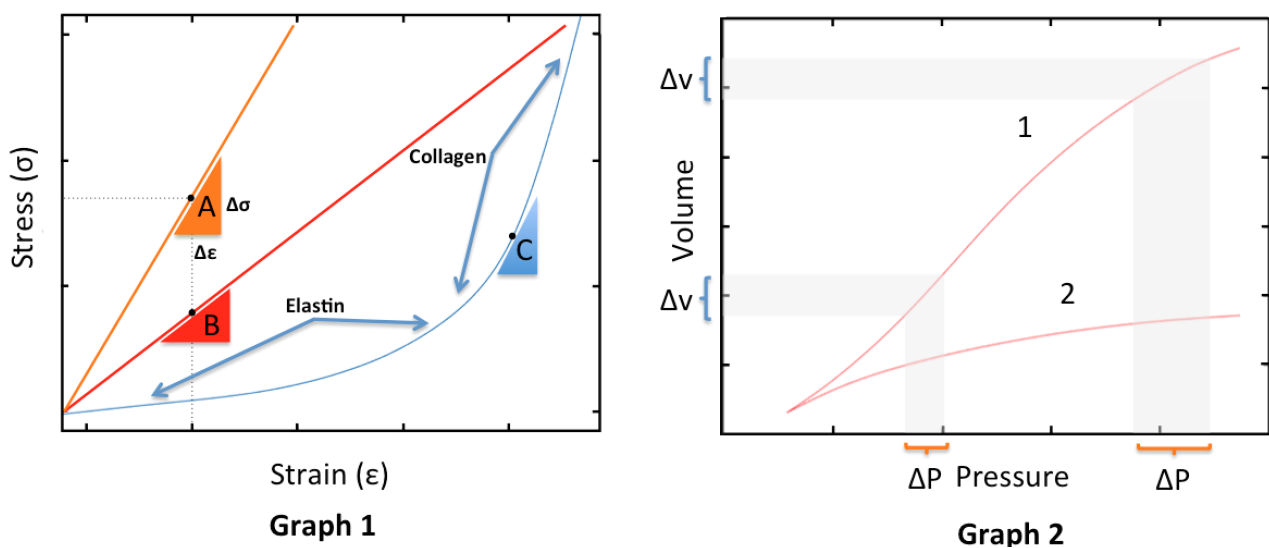


**Figure 6** Graph 1 represents the linear stiffness curves for 2 different materials (material A and material B). Material A has a steeper curve (stiffer material), indicating that for the same deformation (strain) higher degrees of stress are required. Curve C represents the typical stress-strain relationship in biological tissues such as blood vessels and heart. The curve is nonlinear with a typical J-shape. The initial part of the curve is dominated by elastin fibers. The ascending limb of the curve represents the collagen-dominated response that occurs in these tissues at higher stresses. In other words, at higher stresses (pressure), the aorta has a stiffer behavior, with smaller deformations for incrementing stresses.<sup>[28]</sup> Graph 2. Pressure to volume curve ( $\Delta V/\Delta P$ ) representing the typical compliance of arterial tissue in young (curve 1) and in elderly individuals (curve 2). As apparent by both graphs in the above figure, arterial stiffness and compliance are inversely proportional to each other. V, volume. P, pressure.

Computational modeling in cardiovascular medicine offers a unique opportunity to integrate and augment current imaging modalities and to provide tailored and predictive information that can help medical therapy, device development and selection, and surgical planning and intervention<sup>[40]</sup>.

#### Main components of image-based computational fluid dynamics workflow

Patient-specific cardiovascular models are usually constructed from 3D imaging data such as CMR or CT. CFD analysis requires not only information on anatomy but also on physiology (i.e., flow and pressure data) that can be used to set the boundary conditions for the Navier-Stokes equations representing the fluid flow. These equations are solved numerically using a super-computer. We proceed to describe the specific steps of the simulations workflow (Figure 7).

After the acquisition of the image data, the next step is the construction of an anatomical model of the region of interest. This involves delineating the boundaries (e.g., the walls) of the vessels and chambers to be included in the computational analysis using 2D or 3D segmentation techniques. The surfaces of the extracted geometry can be defined either using analytical functions such as b-splines (see panel A figure 8) or discrete surface triangulations that provide a faceted approximation of the surface of the model (see panel B of figure 8). Analytical representations make it possible to create a computer-aided design (CAD) prototype of the anatomical model. On the other hand, surface triangulations are lightweight and can be used to make 3D-printed prototypes of the anatomy.

Multiple manual to semi-automated computer software are available to perform the image segmentation and model creation tasks, with variable degree of user-interaction. Generally speaking, direct-3D segmentation methods (see panel B figure 8) require a smaller user interaction and work well if the quality of the image data is high. These direct-3D methods usually produce a discrete surface triangulation representation of the anatomy<sup>[41]</sup>. Conversely, 2D segmentation methods involve a higher degree of user interaction, but make it possible to handle noisier data. The end result is often an analytical (e.g., non-uniform rational b-spline, NURBS) representation of the model (see panel A figure 8). Analytical models have a significant advantage in CFD simulation over discrete models as they effectively have an unlimited resolution. Conversely, discretized models have a limited resolution given by the point density of the faceted representation of the boundary.

Once the geometry of the model is defined, it must be discretized into a computational mesh. The volume of the geometry is broken down into a collection of cells (also known as elements) and nodes (also known as points). The elements can be of different shapes such as tetrahedral or hexahedral. The equations of motion are then discretized and solved in every element and node of the mesh. Since the mesh has typically hundreds of thousands of elements, the resulting problem has a large number of unknowns, and must be solved using a powerful super-computer. For instance, in Navier-Stokes, every node of the mesh contains four unknowns: the scalar value of pressure, and the three different components of the velocity field.

In the computer modeling paradigm, it is critical to ensure that the obtained numerical solution is “grid-independent”: This means that the same solution is obtained in different meshes, thereby attaining spatial and temporal convergence. A good computational modeling practice is therefore to perform mesh-independence studies, where solutions are obtained in finer and finer computational grids until no change is observed between repeated simulations<sup>[32]</sup>. Figure 9 illustrates an example of different meshes used for mesh-independence analysis in a thoracic aortic flow problem.

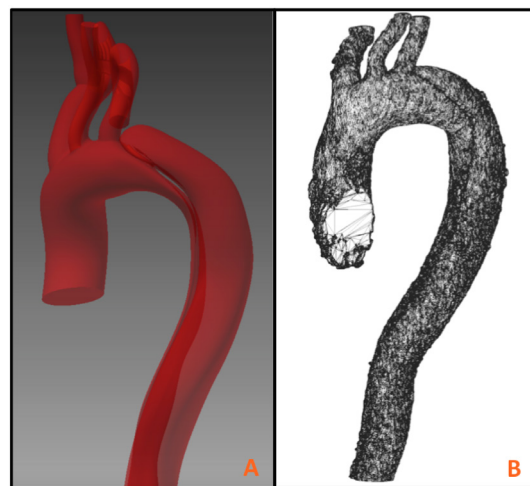


**Figure 8** Two different representations of the same anatomical model of a type B aortic dissection. Panel A depicts a smooth, analytical representation of the segmentation given by NURBS, obtained using 2D segmentation and lofting techniques<sup>[41]</sup>. Panel B shows a surface triangulation of the same data, obtained with direct-3D segmentation techniques.

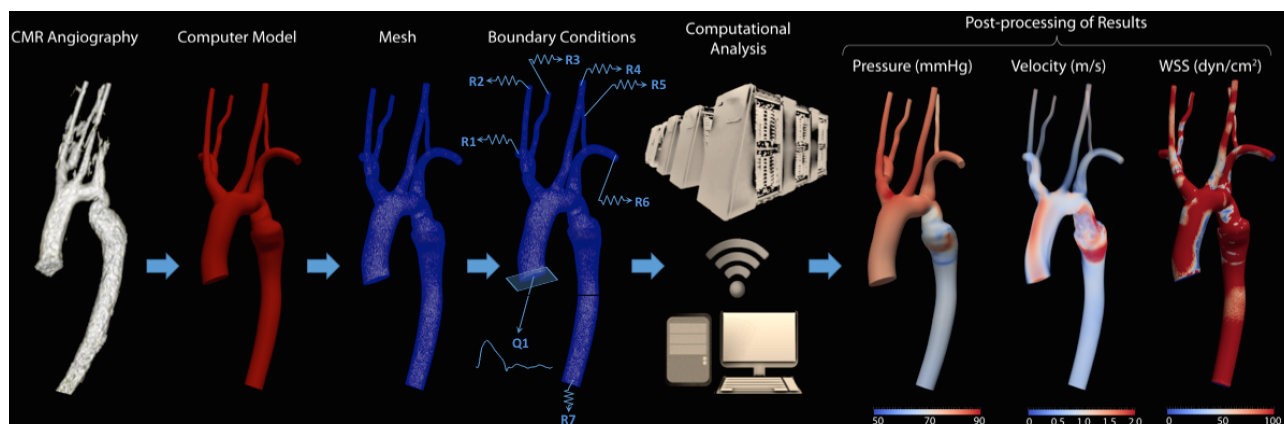


**Figure 7** Example of a CFD simulation on an aortic coarctation case. The acquired raw data is segmented to produce the geometry of the model that is then meshed. After assigning the boundary conditions (Q1, inflow boundary condition given for instance by 2D phase-contrast CMR at the aortic valve; R1-R7 outlet resistors), the computational analysis using a HPC is performed. This enables to map pressure, flow (velocity) and wall shear stress in any point of the 3D model. Of note, only by solving the Navier-Stokes equations can the complex flow patterns and pressure changes shown in the post-stenotic aneurysm be accurately assessed.



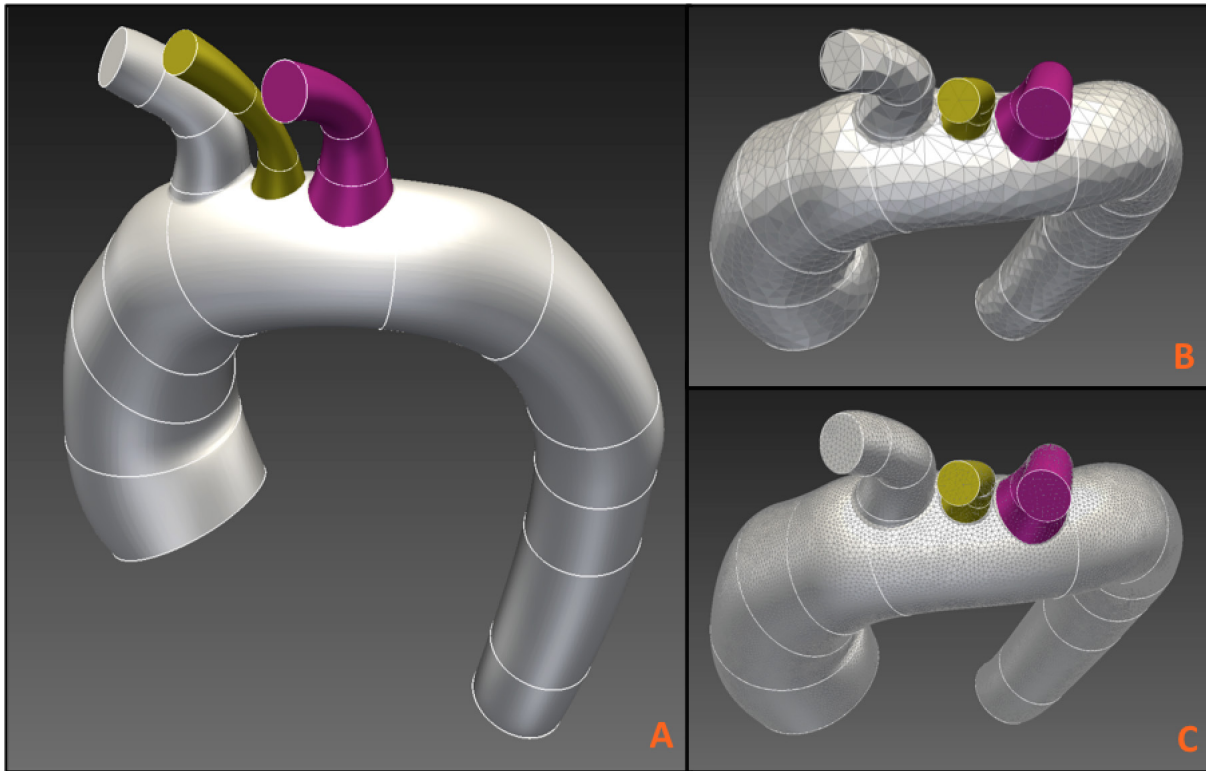


**Figure 9** Panel A. Analytical representation of a thoracic aorta segmentation obtained from a 3D balanced steady-state free precession CMR dataset. Panel B. Coarse computational grid created by assigning a large tetrahedron size. Panel C. Refined computational grid created by reducing the tetrahedral element size used in Panel B.

Once the mesh is created, one must define the so-called “boundary conditions” of every face of the computational model. These conditions are given by measurements (e.g., data) on flow, pressure, wall motion, cardiac function, etc. that provide information for quantities such as cardiac output, flow splits, and microcirculatory resistance. A commonly used approach is to specify flow waveforms at the inflow faces of the computational model, and Windkessel models at the outflow faces. The vessel walls are either modeled as rigid (e.g., a zero velocity is used as a boundary condition), or they are assigned elastic properties derived from wall motion data. Figure 10 provides a schematic of typical boundary conditions used in aortic flow modeling.

The final step in the simulation workflow involves obtaining the numerical solution for the equations representing the laws of fluid dynamics (e.g., Navier-Stokes) at each point of the computational mesh using HPC and powerful algorithms. Once the solution is obtained, it is post-processed to visualize fields such as velocity, pressure, WSS, etc. (see figure 7). Ultimately, CFD provides a high-resolution description of 3D physics of flow (e.g., 3D velocities and pressures at every point of the computational grid) by having a small number of physiological measurements (e.g., phase-contrast or Doppler flow, catheter-derived pressure, etc.) at a small number of locations.

## ADVANCED IMAGE-BASED DECISION SUPPORT: CASE-SPECIFIC EXAMPLES

Quantification of quantities such as blood flow velocity, WSS and pressure is critical in the assessment, treatment planning, and management of patients with congenital and acquired cardiovascular disease as described before. In this section we present some examples on how computational modeling can give valuable insights and change our approach in two common congenital malformations.

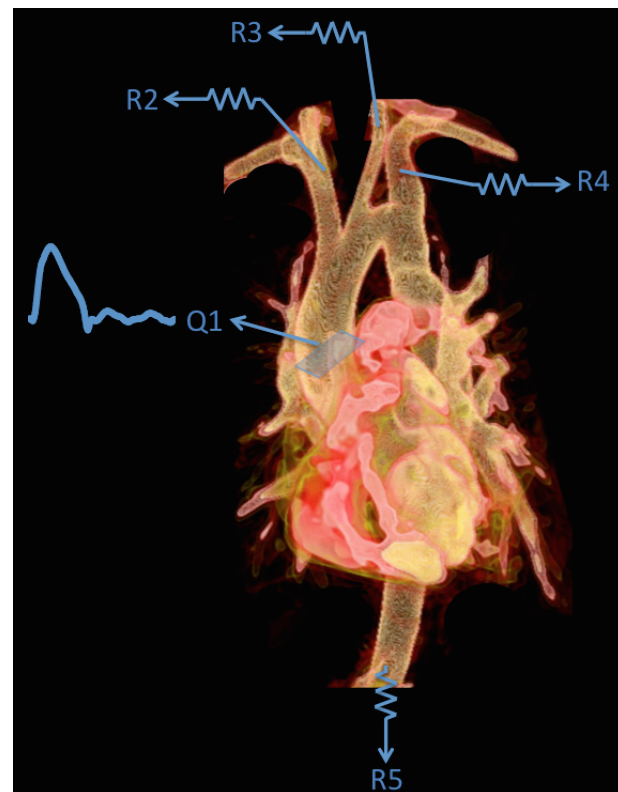


**Figure 10** Volume-rendered 3D geometry from a time-resolved magnetic resonance angiography acquired in a 26 year-old aortic coarctation patient with previous patch aortoplasty repair and residual re-coarctation. Representation of the boundary conditions required for solving the velocity and pressure fields in the aorta using computational fluid dynamics. This model has an inflow (Q1) defined by 2D phase-contrast CMR flow data. R1 to R5 represent the resistors imposed at each of the outlet faces of the model.



## 1. Aortic coarctation

CoA is a narrowing of the aorta, almost always located at the junction of the distal aortic arch and the descending aorta, at the insertion of the ductus arteriosus or just distal to the left subclavian artery origin. It can be a localized stenosis or a more diffuse form characterized by a longer hypoplastic segment. It may also occur as an isolated defect (simple CoA) or in association with other intra/extra-cardiac malformations (complex CoA) (Figure 11). It accounts for up to 8% of all CHD, with a reported prevalence in the simple forms of about 3 per 10,000 live births<sup>[42,43]</sup>.

Importantly, often regarded as a localized anatomical obstruction, CoA is a complex cardiovascular disorder associated with a diffuse and lifelong arteriopathy that persists even after corrective intervention at an early age<sup>[42,43]</sup>. These patients show reduced survival even after coarctectomy is performed compared with their unaffected aged-matched peers. Besides factors such as hemodynamic status at the time of surgery, survival is also significantly affected by age at operation, therefore early repair has been advocated.

Systemic hypertension has a prevalence ranging from 19% early after repair up to 68% in long-term follow-up studies in adults. It is one of the most important contributing factors to the increased cardiovascular mortality in repaired CoA patients. Extreme blood pressure rises in response to exercise have also recently been shown to predict late onset hypertension, with some authors advocating exercise testing to detect residual aortic arch gradients in these patients<sup>[43,44]</sup>.

Although the etiology of hypertension after early CoA repair is still not entirely understood, it is likely determined by an interplay of multiple factors including valve (bicuspid valve occurs in up to 85% of cases) and arch morphology, re-coarctation, endothelial dysfunction and vascular stiffness, as well as impaired mechanical properties of large conduit vessels<sup>[44-46]</sup>.

It has been described that structural abnormalities in the aortic media (medial degeneration with early elastic fiber fragmentation and fibrosis) result in an increased stiffness of the aorta and the carotid arteries. This is likely explained by the proliferation of collagen and degradation of elastin fibers, resulting in an overall stiffer vessel (see graph 1 of figure 6), in a blunted baroreceptor reflex, and in an increased brachial pulse wave velocity. These changes have been related to late aneurysm formation and aortic dissection.

Vascular stiffness on the other hand, is known to accelerate hypertension, and in turn, hypertension leads to greater arterial stiffness<sup>[47]</sup>. However, the mechanisms that explain the relationship between arterial stiffness and hypertension are still not entirely understood. There is conventional assumption that hypertension stimulates aortic remodeling and stiffening as an adaptive process according to Laplace's Law<sup>[48]</sup>. However, a recent longitudinal study demonstrated that arterial stiffness actually precedes an increase in systolic blood pressure and newly diagnosed hypertension<sup>[49]</sup>.

Hypertension has been extensively correlated with end-organ damage, from premature coronary atherosclerosis and cerebrovascular disease, to compensatory LV hypertrophy at an early stage in response to an increase in afterload, diastolic and systolic dysfunction. This interaction between the vascular dysfunction and the LV (ventriculo-arterial coupling) is an area of active research<sup>[44]</sup>. Experimental and clinical studies have also shown that hypertension causes not only LV but also arterial remodeling<sup>[50]</sup>. This remodeling (e.g., medial thickening in response to elevated pressure loads) is again consistent with Laplace's law (Figure 5) as discussed before. It is thought that circumferential stress is likely to be a major contributing factor in the remodeling effects of hypertension<sup>[51]</sup>.

Recent work using CMR image-based CFD simulation in CoA



**Figure 11** Example of a volume-rendered 3D geometry from a cardiac CT study acquired in a newborn with complex severe coarctation (blue arrow). Segmental analysis confirmed tricuspid atresia, ventriculo-arterial discordance with the aorta arising from the hypoplastic right ventricle and severe aortic coarctation with ductal continuation of the descending aorta.

patients treated with resection and end-to-end anastomosis revealed disrupted WSS indices in the descending aorta. These altered WSS indices correlate with high incidence of plaque formation in that region<sup>[52]</sup>. A reliable estimation of WSS in the aorta requires an accurate 3D reconstruction of the anatomy, knowledge of the blood viscosity and detailed characterization of the blood velocity. Furthermore, assessment of peak wall stress ( $PWS = \max T_{\theta} = P_{\max} r/h$ , see figure 5) is particularly relevant since there is also significant evidence of its correlation with the atherogenic process. PWS is also a reliable parameter to assess the future risk of rupture of aneurysms, more reliable than maximum transverse diameter<sup>[53,54]</sup>.

To be able to accurately assess the so called “fifth chamber of the heart” and study and monitor the interaction between the aorta damping of the ventricular pulse wave and the LV, we need to be able to perform non-invasive characterization of biomechanical properties of both the ventricular and vascular walls. We are now able to measure non-invasively the local and global mechanical properties of a vessel such as vascular stiffness, a sensitive and useful biomarker of cardiovascular risk<sup>[55,56]</sup>, based on 3D fluid-structure interaction models and the full aortic wall motion data obtained from dynamic 3D volume datasets. This is a major advantage over the commonly used methods used to estimate average arterial stiffness (pulse wave velocity by solving the Moens-Korteweg equation or vascular elastography), based on simplified models that conceptualize a pressure wave composed of one single forward wave and one single reflected wave, originating from a single reflection site<sup>[57]</sup>.

Additionally, we are now able to accurately predict the non-invasive pressure gradient across the coarctation site without the limitations of using simplified assumptions to estimate it (e.g. when using the modified Bernoulli's equation in echocardiography) with a good agreement with the invasive diagnostic catheter investigation and simulate the aortic hemodynamics during stress testing<sup>[58]</sup>.

## 2. Peripheral pulmonary stenosis

Narrowing of the branch pulmonary arteries can occur as an isolated defect but it is often associated with other conditions such as Tetralogy of Fallot (Figure 12), Williams's syndrome or other elastin defi-

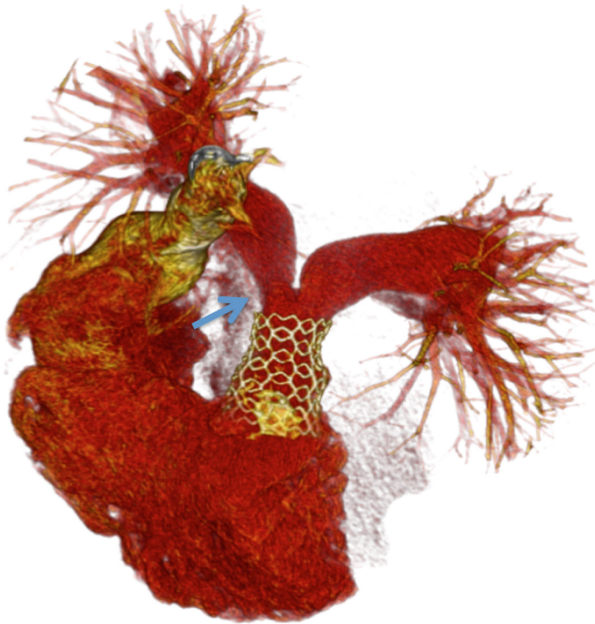


**Figure 12** Volume-rendered 3D geometry from a CT pulmonary angiogram acquired in a 24 year-old patient with Tetralogy of Fallot and a pulmonary stent, with moderate stenosis of the right pulmonary artery (blue arrow).

ciencies, Alagille's syndrome, or may represent long-term sequelae even after successful repair (e.g., LeCompte maneuver for transposition of the great arteries, post-Glenn, etc.). Although this obstruction to flow can ultimately cause elevated right ventricular (RV) pressure, compensatory RV hypertrophy, and in severe cases RV failure, conflicting data from small series and anecdotal cases suggests that peripheral pulmonary stenosis might actually improve over time without intervention<sup>[59,60]</sup>.

Transcatheter angioplasty and stent implantation has matured over the past decade into a safe and accepted treatment for patients with hemodynamically significant stenosis. In fact, the increase in vessel luminal area after percutaneous treatment has shown not only to improve acute outcomes through a decrease in RV pressure (reduced RV:aortic pressure ratio), but also to reduce chronic RV pressure overload and mortality in the long term<sup>[59]</sup>. However, data is still scarce, based on small retrospective cohorts and therefore not allowing extrapolation to all patients with significant peripheral pulmonary stenosis (PPS).

The current paradigm for intervention planning in these patients still relies exclusively on detailed anatomic and physiologic diagnostic data from non-invasive and invasive modalities (echocardiography or CMR/CT and cardiac catheterization) to define the severity of stenosis. Despite the accuracy of these investigations, they do not to predict the treatment outcome due to individual variability and complexity of human biological systems<sup>[61]</sup>.

Patient-specific computational modeling can provide valuable insight and help guide pre-intervention planning in these patients. Interesting data has been published on a patient with unilateral PPS using a nonlinear, one-dimensional image-based model of the proximal pulmonary arteries and impedance models of the pulmonary microvasculature fitted to morphometric data<sup>[62]</sup>. The study investigated changes in pulmonary flow and pressure following virtual removal of the stenosis. For that particular case, it was found that the correction of the anatomical obstruction resulted in negligible changes in blood flow and pressure<sup>[62]</sup>.

These results suggest that the persistence of the stenosis precludes normal lung development and therefore results in few and smaller vessel branches to the affected side, which has a much higher peripheral vascular resistance. Indeed, it is known that the major determinants of pulmonary blood flow are the topology of the vascular bed, the pressures of alveolar gas in alveoli and blood, the viscosity of blood, the elasticity of the blood vessels and the intrapleural pressure<sup>[63]</sup>. Since pressure is a force ( $F$ ) per unit area ( $A$ ) ( $P = F/A$ ), the larger the total cross-sectional area the lower the pressure. Furthermore, according to Poiseuille's law, the smaller the capillary bed the higher the vascular resistance in the lung supplied by the stenotic pulmonary artery.

However, there are numerous examples in the clinical literature in which the effectiveness of transcatheter therapy for PPS has been demonstrated. A general deficiency in any case, however, is the small size and the retrospective nature of the available evidence<sup>[59,64-67]</sup>.

The key message from these studies is that there is a pressing need to incorporate physiological/functional-based measurements into the anatomical assessment of occlusive disease, even if 3D curved multiplanar reformatted projections are used. This is particularly relevant if the expected hemodynamic benefits are minimal to justify the potential risks of the procedure. Although a persistent obstruction is likely to precipitate clinical deterioration, what these studies are highlighting is the need of early intervention, before vascular remodeling entrenches, thus limiting any clinical benefit to the patient.

An analogy can be applied to the more common coronary artery stenosis scenario and the role of stress testing in the functional assessment both in the pre and post-coronary revascularization settings, or the unresolved conundrum of optimal management of stable coronary artery disease following the landmark multicenter randomized trials COURAGE, FAME 2 and BARI 2D<sup>[66,68]</sup>. The use of non-invasive estimation of fraction flow reserve, the proportion of flow across a stenosis measured as a ratio between pressures proximal and distal to the stenotic lesion, at maximal hyperemia, using CT angiography and CFD to predict the hemodynamic significance of coronary lesions, is just another application with a growing body of evidence<sup>[69-71]</sup>.

## PRESENT AND FUTURE CHALLENGES

Advances in cross-sectional cardiovascular imaging, integrated imaging processing/segmentation platforms, and increased availability of high-speed super-computers to solve complex computational models of fluid dynamics have made it possible to obtain anatomically and physiologically realistic models of time-varying 3D hemodynamics. The ability to simulate both resting and stress conditions can provide unique insights into the physics of blood flow patterns, uncover normal and abnormal physiologic responses or residual problems, further enhancing our knowledge about the pathophysiology of different diseases. In fact, because often changes in cardiac function can only be revealed during exercise, stress testing has increasingly become part of the risk assessment in the follow-up of patients with CHD, both prior and after surgical correction<sup>[72]</sup>. Together with the clinical assessment, these patient-specific simulations can further support and personalize patient management.

The CFD workflow has numerous steps, as described in figure 7. In some applications, CFD simulations can be run efficiently, reliably and quickly using multi-core commercially available processors. However, large-scale problems still require HPC hardware, whose access is still limited to bioengineers, scientists and academics.

It is beyond the scope of this manuscript to discuss the numerous

commercial and open-source codes available to perform the tasks of medical image data segmentation, surface and volumetric mesh generation, and simulation of flow. It is important to underline that, whichever tool is used, the geometry segmentation is a critical and generally very user-dependent operation, which may affect decisively the outcome of the analysis. New image-to-computation algorithms have been proposed to minimize the degree of user-intervention in the definition of the geometry<sup>[73]</sup>.

CFD studies may also be limited by the lack of patient-specific information on certain properties that must be inferred from population-based studies. Yet, modeling is about making reasonable assumptions and using indirect measurements of quantities that cannot be directly assessed. This is in fact one of the main strengths of modeling. As an example, artificial neural networks, computational tools for pattern recognition that use learning algorithms built on experience, are already being used in medicine to identify relations in input data that are not easily apparent with more common analytic techniques<sup>[74]</sup>. The construction of a cardiovascular pipeline and collection of library of parameters (cardiovascular statistical atlases and computational models of the heart and vessels) that can be used to quickly predict biomechanics/fluid behavior in a population level is an area of active research, with the potential to reveal new cardiovascular biomechanic metrics and provide novel insights into certain diseases<sup>[75]</sup>.

Additionally, image-based modeling is fundamentally affected by limitations in the temporal-spatial resolution of the acquired image data, particularly in small-sized structures and patients with smaller body-surface-areas.

New software platforms for geometric modeling should also provide more clinician-friendly interfaces. Unfortunately, although most commercially available solutions for 3D medical imaging post-processing provide critical information for surgical planning, complex clinical decision-making and patient follow-up, their outputs are not easy to adapt to the CFD workflow.

Furthermore, open debates between bioengineers and clinicians about the role of CFD in cardiovascular medicine might help bring more awareness to the medical community to this growing field. Future clinicians should be aware of the benefits that image-based modeling can bring to their clinical practice. This will help to create new opportunities to bring modeling into the clinic.

#### *Critical Path Initiative*

As described before, CFD is being used routinely for development and assessment of cardiovascular devices (e.g. vascular stents, prosthetic heart valves, etc.), avoiding costly experimental prototypes by providing “in vitro” insight into their performance. However, guidance documents on best practice, CFD training programs and certification, and adequate review of the application of this predictive computational modeling is still lacking.

To address this deficiency, the Food and Drug Administration (FDA) has recently launched an initiative to standardize CFD techniques used among different laboratories. This FDA-sponsored project evaluated the use and limitations of CFD in assessing blood flow parameters related to medical device safety. It brought together academia, industry, and the FDA to address the need for adequate and systematic validation of the use of CFD for pre-market device applications and post-market investigations.

The international CFD community was invited to perform independent simulations of a simple benchmark problem containing features commonly encountered in medical devices. This inter-laboratory study included experienced participants from 28 different

groups and highlighted a significant amount of measurement error and variability in flow measurements. Despite the general disappointment, these results helped to delineate a standard operating procedure and a list of best practices that will be the cornerstone to increase the reliability of CFD analyses and to maintain uniformity among researchers<sup>[76]</sup>.

## CONCLUSION

CFD has emerged and is maturing into a unique tool that, together with basic experimentation, can provide insights of unprecedented detail into the biomechanics of blood flow and its relation to the heart and vascular system in CHD.

High-quality patient-specific 3D biomedical data are the sine qua non condition to make a reality the paradigm of personalized medicine in CHD through CFD simulation. Using individualized geometry and limited physiological data, researchers are able to perform computational analysis to determine and predict relevant biophysical properties unique to that patient.

The lack of multiscale models to represent the intricate nature of cardiovascular pathophysiology currently represents a major limitation of most simulations. Even though the individual prognosis/response to a specific treatment cannot be entirely predicted from computational modeling one may argue that this patient-specific data might have advantages over population-based clinical decision making.

Although there is still a long way to go, tailored medical treatment based on such simulations has already had major impact in cardiovascular medicine. In fact, this knowledge is already used to customize medical devices such as vascular stents less prone to restenosis, to understand the hemodynamics of heart valves that lead to thrombo-embolic complications or early structural failure via sophisticated fluid dynamics testing<sup>[77]</sup>. Additionally, CFD has provided a unique insight into the biomechanical adaptations in certain diseases, such as CoA, refocusing not on the anatomical problem but on the diffuse nature of the disease and the importance of the individualized timing for intervention.

Closer links between bioengineers, researchers and clinicians, together with CFD training and certification (including clinicians), better access to HPC and more clinician-friendly platforms to perform the simulations are needed. Finally, for CFD simulations to gain further confidence from the medical community they must also undergo comprehensive validation with experimental data and certification, and these patient-specific simulations must be informative within clinically relevant time scales.

## ACKNOWLEDGMENTS

The authors acknowledge support from the European Research Council under the European Union's Seventh Framework Programme (FP/2007-2013) / ERC Grant Agreement n. 307532, BHF New Horizons program (NH/11/5/29058), and the United Kingdom Department of Health via the National Institute for Health Research (NIHR) comprehensive Biomedical Research Centre award to Guy's & St Thomas' NHS Foundation Trust in partnership with King's College London and King's College Hospital NHS Foundation Trust."

## CONFLICT OF INTERESTS

There are no conflicts of interest with regard to the present study.



## REFERENCES

- Reid, G.J., et al., Estimates of life expectancy by adolescents and young adults with congenital heart disease. *J Am Coll Cardiol*, 2006. 48(2): p. 349-55.
- Opatowsky, A.R., O.K. Siddiqi, and G.D. Webb, Trends in hospitalizations for adults with congenital heart disease in the U.S. *J Am Coll Cardiol*, 2009. 54(5): p. 460-7.
- Warnes, C.A., et al., ACC/AHA 2008 guidelines for the management of adults with congenital heart disease: a report of the American College of Cardiology/American Heart Association Task Force on Practice Guidelines (Writing Committee to Develop Guidelines on the Management of Adults With Congenital Heart Disease). Developed in Collaboration With the American Society of Echocardiography, Heart Rhythm Society, International Society for Adult Congenital Heart Disease, Society for Cardiovascular Angiography and Interventions, and Society of Thoracic Surgeons. *J Am Coll Cardiol*, 2008. 52(23): p. e143-263.
- Baumgartner, H., et al., ESC Guidelines for the management of grown-up congenital heart disease (new version 2010). *Eur Heart J*, 2010. 31(23): p. 2915-57.
- Silversides, C.K., et al., Canadian Cardiovascular Society 2009 Consensus Conference on the management of adults with congenital heart disease: executive summary. *Can J Cardiol*, 2010. 26(3): p. 143-50.
- Ernest, T.B., et al., Developing paediatric medicines: identifying the needs and recognizing the challenges. *J Pharm Pharmacol*, 2007. 59(8): p. 1043-55.
- Valsangiacomo Buechel, E.R., et al., Indications for cardiovascular magnetic resonance in children with congenital and acquired heart disease: an expert consensus paper of the Imaging Working Group of the AEPC and the Cardiovascular Magnetic Resonance Section of the EACVI. *Cardiol Young*, 2015: p. 1-20.
- Bergersen, L., et al., Adverse event rates in congenital cardiac catheterization - a multi-center experience. *Catheter Cardiovasc Interv*, 2010. 75(3): p. 389-400.
- Ntsinjana, H.N., M.L. Hughes, and A.M. Taylor, The role of cardiovascular magnetic resonance in pediatric congenital heart disease. *J Cardiovasc Magn Reson*, 2011. 13: p. 51.
- Sodian, R., et al., Stereolithographic models for surgical planning in congenital heart surgery. *Ann Thorac Surg*, 2007. 83(5): p. 1854-7.
- Nagueh, S.F., et al., Recommendations for the evaluation of left ventricular diastolic function by echocardiography. *J Am Soc Echocardiogr*, 2009. 22(2): p. 107-33.
- Garcia, D., et al., Two-Dimensional Intraventricular Flow Mapping by Digital Processing Conventional Color-Doppler Echocardiography Images. *Ieee Transactions on Medical Imaging*, 2010. 29(10): p. 1701-1713.
- Janda, S., et al., Diagnostic accuracy of echocardiography for pulmonary hypertension: a systematic review and meta-analysis. *Heart*, 2011. 97(8): p. 612-22.
- Greiner, S., et al., Reliability of noninvasive assessment of systolic pulmonary artery pressure by Doppler echocardiography compared to right heart catheterization: analysis in a large patient population. *J Am Heart Assoc*, 2014. 3(4).
- Tschope, C. and W.J. Paulus, Is echocardiographic evaluation of diastolic function useful in determining clinical care? Doppler echocardiography yields dubious estimates of left ventricular diastolic pressures. *Circulation*, 2009. 120(9): p. 810-20; discussion 820.
- Gomez, A., et al., 3D Intraventricular Flow Mapping from Colour Doppler Images and Wall Motion. *Medical Image Computing and Computer-Assisted Intervention - Miccai 2013, Pt Ii*, 2013. 8150: p. 476-483.
- Johnson, J.N., et al., Cumulative radiation exposure and cancer risk estimation in children with heart disease. *Circulation*, 2014. 130(2): p. 161-7.
- Maurovich-Horvat, P., et al., Comprehensive plaque assessment by coronary CT angiography. *Nat Rev Cardiol*, 2014. 11(7): p. 390-402.
- Taylor, C.A., T.A. Fonte, and J.K. Min, Computational fluid dynamics applied to cardiac computed tomography for noninvasive quantification of fractional flow reserve: scientific basis. *J Am Coll Cardiol*, 2013. 61(22): p. 2233-41.
- Choy, J.S. and G.S. Kassab, Scaling of myocardial mass to flow and morphometry of coronary arteries. *J Appl Physiol* (1985), 2008. 104(5): p. 1281-6.
- Hundley, W.G., et al., Quantitation of Cardiac-Output with Velocity-Encoded, Phase-Difference Magnetic-Resonance-Imaging. *American Journal of Cardiology*, 1995. 75(17): p. 1250-1255.
- Reiter, G., et al., Magnetic resonance-derived 3-dimensional blood flow patterns in the main pulmonary artery as a marker of pulmonary hypertension and a measure of elevated mean pulmonary arterial pressure. *Circ Cardiovasc Imaging*, 2008. 1(1): p. 23-30.
- Andersson, B., *Computational fluid dynamics for engineers*. 2012, Cambridge; New York: Cambridge University Press. xi, 189 p.
- Prasad, A., et al., A computational framework for investigating the positional stability of aortic endografts. *Biomech Model Mechanobiol*, 2013. 12(5): p. 869-87.
- Sagawa, K., R.K. Lie, and J. Schaefer, Translation of Frank, Otto Paper the Basic Shape of the Arterial Pulse - 1st Treatise - Mathematical-Analysis - Translators Introduction. *Journal of Molecular and Cellular Cardiology*, 1990. 22(3): p. 253-254.
- Westerhof, N., J.W. Lankhaar, and B.E. Westerhof, The arterial Windkessel. *Med Biol Eng Comput*, 2009. 47(2): p. 131-41.
- Wesseling, K.H., et al., Computation of aortic flow from pressure in humans using a nonlinear, three-element model. *J Appl Physiol* (1985), 1993. 74(5): p. 2566-73.
- Wagenseil, J.E. and R.P. Mecham, Elastin in Large Artery Stiffness and Hypertension. *Journal of Cardiovascular Translational Research*, 2012. 5(3): p. 264-273.
- Nichols WW, O'Rourke MF, Charalambos V. (2011) McDonald's blood flow in arteries: theoretical, experimental and clinical principles. London: Hodder Arnold.
- Tu J, Yeoh GH, Liu C. (2013) *Computational Fluid Dynamics*. Amsterdam: Butterworth-Heinemann.
- Gonzalez, C.F., et al., Intracranial Aneurysms - Flow-Analysis of Their Origin and Progression. *American Journal of Neuroradiology*, 1992. 13(1): p. 181-188.
- Taylor, C.A. and C.A. Figueroa, Patient-specific modeling of cardiovascular mechanics. *Annu Rev Biomed Eng*, 2009. 11: p. 109-34.
- Sun, Z. and L. Xu, Computational fluid dynamics in coronary artery disease. *Comput Med Imaging Graph*, 2014. 38(8): p. 651-63.
- Gundert, T.J., et al., Optimization of Cardiovascular Stent Design Using Computational Fluid Dynamics. *Journal of Biomechanical Engineering-Transactions of the Asme*, 2012. 134(1).
- Dubini, G., et al., Ten years of modelling to achieve haemodynamic optimisation of the total cavopulmonary connection. *Cardiol Young*, 2004. 14 Suppl 3: p. 48-52.
- Hsia, T.Y., et al., Use of Mathematical Modeling to Compare and Predict Hemodynamic Effects Between Hybrid and Surgical Norwood Palliations for Hypoplastic Left Heart Syndrome. *Circulation*, 2011. 124(11): p. S204-S210.
- Chetan, D., et al., Surgical Palliation Strategy Does Not Affect Interstage Ventricular Dysfunction or Atrioventricular Valve Regurgitation in Children With Hypoplastic Left Heart Syndrome and Variants. *Circulation*, 2013. 128(11): p. S205-S212.
- Migliavacca, F., et al., Multiscale modelling in biofluidynamics: Application to reconstructive paediatric cardiac surgery. *Journal of Biomechanics*, 2006. 39(6): p. 1010-1020.
- Marsden, A.L., *Optimization in Cardiovascular Modeling*. Annual



- Review of Fluid Mechanics, Vol 46, 2014. 46: p. 519-546.
40. Koo, B.K., et al., Diagnosis of Ischemia-Causing Coronary Stenoses by Noninvasive Fractional Flow Reserve Computed From Coronary Computed Tomographic Angiograms Results From the Prospective Multicenter DISCOVER-FLOW (Diagnosis of Ischemia-Causing Stenoses Obtained Via Noninvasive Fractional Flow Reserve) Study. *Journal of the American College of Cardiology*, 2011. 58(19): p. 1989-1997.
41. Dillon-Murphy D, Noorani A, Nordsletten D, Figueroa CA. Multimodality image-based computational analysis of haemodynamics in aortic dissection. *Biomech Model Mechanobiol*. 2015 Sep 28. [Epub ahead of print]
42. Hoffman, J.I.E. and S. Kaplan, The incidence of congenital heart disease. *Journal of the American College of Cardiology*, 2002. 39(12): p. 1890-1900.
43. Vriend, J.W.J. and B.J.M. Mulder, Late complications in patients after repair of aortic coarctation: implications for management. *International Journal of Cardiology*, 2005. 101(3): p. 399-406.
44. O'Sullivan, J., Late Hypertension in Patients with Repaired Aortic Coarctation. *Current Hypertension Reports*, 2014. 16(3).
45. Roos-Hesselink, J.W., et al., Aortic valve and aortic arch pathology after coarctation repair. *Heart*, 2003. 89(9): p. 1074-7.
46. Warnes, C.A., Bicuspid aortic valve and coarctation: two villains part of a diffuse problem. *Heart*, 2003. 89(9): p. 965-966.
47. Franklin, S.S., et al., Hemodynamic patterns of age-related changes in blood pressure. The Framingham Heart Study. *Circulation*, 1997. 96(1): p. 308-15.
48. Gibbons, G.H. and V.J. Dzau, The emerging concept of vascular remodeling. *N Engl J Med*, 1994. 330(20): p. 1431-8.
49. Kaess, B.M., et al., Aortic stiffness, blood pressure progression, and incident hypertension. *JAMA*, 2012. 308(9): p. 875-81.
50. Mayet, J. and A. Hughes, Cardiac and vascular pathophysiology in hypertension. *Heart*, 2003. 89(9): p. 1104-9.
51. Roman, M.J., et al., Parallel cardiac and vascular adaptation in hypertension. *Circulation*, 1992. 86(6): p. 1909-18.
52. LaDisa, J.F.J., et al., Computational Simulations Demonstrate Altered Wall Shear Stress in Aortic Coarctation Patients Treated by Resection with End-to-end Anastomosis. *Congenital Heart Disease*, 2011. 6(5): p. 432-443.
53. Fillinger, M.F., et al., Prediction of rupture risk in abdominal aortic aneurysm during observation: wall stress versus diameter. *J Vasc Surg*, 2003. 37(4): p. 724-32.
54. Katritsis, D., et al., Wall shear stress: theoretical considerations and methods of measurement. *Prog Cardiovasc Dis*, 2007. 49(5): p. 307-29.
55. Wang, X., et al., Assessment of arterial stiffness, a translational medicine biomarker system for evaluation of vascular risk. *Cardiovasc Ther*, 2008. 26(3): p. 214-23.
56. Blacher, J. and M.E. Safar, Large-artery stiffness, hypertension and cardiovascular risk in older patients. *Nature Clinical Practice Cardiovascular Medicine*, 2005. 2(9): p. 450-455.
57. Segers P, K.J., Tracheta B, Swillens A, Vermeersch Sebastian, Mahieub Dries, Rietzschelc Ernst, De Buyzerec Marc, Van Bortelb Luc Limitations and pitfalls of non-invasive measurement of arterial pressure wave reflections and pulse wave velocity. *Artery Research*, 2009. 3(2): p. 79-88.
58. Sotelo JA, U.J., Valverde I, Tejos C, Irrarazaval P, Hurtado DE, and Uribe S, 3D quantification of hemodynamics parameters of pulmonary artery and aorta using finite-element interpolations in 4D flow MR data. *Journal of Cardiovascular Magnetic Resonance*, 2015. 17((Suppl 1)): p. Q27
59. Cunningham, J.W., et al., Outcomes After Primary Transcatheter Therapy in Infants and Young Children With Severe Bilateral Peripheral Pulmonary Artery Stenosis. *Circulation-Cardiovascular Interventions*, 2013. 6(4): p. 460-467.
60. Wessel, A., et al., Three decades of follow-up of aortic and pulmonary vascular lesions in the Williams-Beuren syndrome. *Am J Med Genet*, 1994. 52(3): p. 297-301.
61. Taylor, C.A., et al., Predictive medicine: computational techniques in therapeutic decision-making. *Comput Aided Surg*, 1999. 4(5): p. 231-47.
62. Spilker, R.L., et al., Morphometry-based impedance boundary conditions for patient-specific modeling of blood flow in pulmonary arteries. *Annals of Biomedical Engineering*, 2007. 35(4): p. 546-559.
63. Fung, Y.c., *Biomechanics: Circulation* 2nd ed. 1997, New York: Springer Science.
64. Oyen, W.J., et al., Pulmonary perfusion after endovascular stenting of pulmonary artery stenosis. *J Nucl Med*, 1995. 36(11): p. 2006-8.
65. Bacha, E.A. and J. Kreutzer, Comprehensive management of branch pulmonary artery stenosis. *J Interv Cardiol*, 2001. 14(3): p. 367-75.
66. Lynch, W., et al., Hybrid branch pulmonary artery stent placement in adults with congenital heart disease. *Interact Cardiovasc Thorac Surg*, 2015. 20(4): p. 499-503.
67. Fogelman, R., et al., Endovascular stents in the pulmonary circulation. Clinical impact on management and medium-term follow-up. *Circulation*, 1995. 92(4): p. 881-5.
68. Group, B.D.S., et al., A randomized trial of therapies for type 2 diabetes and coronary artery disease. *N Engl J Med*, 2009. 360(24): p. 2503-15.
69. Min, J.K., et al., Diagnostic accuracy of fractional flow reserve from anatomic CT angiography. *JAMA*, 2012. 308(12): p. 1237-45.
70. Norgaard, B.L., et al., Diagnostic Performance of Noninvasive Fractional Flow Reserve Derived From Coronary Computed Tomography Angiography in Suspected Coronary Artery Disease The NXT Trial (Analysis of Coronary Blood Flow Using CT Angiography: Next Steps). *Journal of the American College of Cardiology*, 2014. 63(12): p. 1145-1155.
71. Koo, B.K., et al., Diagnosis of ischemia-causing coronary stenoses by noninvasive fractional flow reserve computed from coronary computed tomographic angiograms. Results from the prospective multicenter DISCOVER-FLOW (Diagnosis of Ischemia-Causing Stenoses Obtained Via Noninvasive Fractional Flow Reserve) study. *J Am Coll Cardiol*, 2011. 58(19): p. 1989-97.
72. Helbing, W.A., et al., Cardiac stress testing after surgery for congenital heart disease. *Curr Opin Pediatr*, 2010. 22(5): p. 579-86.
73. Dillard, S.I., et al., From medical images to flow computations without user-generated meshes. *International Journal for Numerical Methods in Biomedical Engineering*, 2014. 30(10): p. 1057-1083.
74. Itchhaporia, D., et al., Artificial neural networks: Current status in cardiovascular medicine. *Journal of the American College of Cardiology*, 1996. 28(2): p. 515-521.
75. Broadhouse, K.M., et al., Cardiovascular magnetic resonance of cardiac function and myocardial mass in preterm infants: a preliminary study of the impact of patent ductus arteriosus. *J Cardiovasc Magn Reson*, 2014. 16: p. 54.
76. Hariharan, P., et al., Multilaboratory particle image velocimetry analysis of the FDA benchmark nozzle model to support validation of computational fluid dynamics simulations. *J Biomech Eng*, 2011. 133(4): p. 041002.
77. Yoganathan, A.P., K.B. Chandran, and F. Sotiropoulos, Flow in prosthetic heart valves: State-of-the-art and future directions. *Annals of Biomedical Engineering*, 2005. 33(12): p. 1689-1694.

**Peer reviewers:** Tony Reybrouck, Professor, Department of Cardiovascular Rehabilitation, University Hospitals, Campus Gasthuisberg, Herestraat, 3000 Leuven, Belgium; Narayan Bahadur Basnet, Pediatrics, Pediatric Cardiology, Children's Medical Diagnosis Center (CMDC), Chabahil, Kathmandu-7, Kathmandu, NEPAL.